ACS APPLIED MATERIALS & INTERFACES

Research Article

www.acsami.org

Application of Europium Multiwalled Carbon Nanotubes as Novel Luminophores in an Electrochemiluminescent Aptasensor for Thrombin Using Multiple Amplification Strategies

Dan Wu,[†] Xia Xin,[‡] Xuehui Pang,[†] Marek Pietraszkiewicz,[§] Robert Hozyst,[§] Xian′ge Sun,[†] and Qin Wei*[,†]

[†]Key Laboratory of Chemical Sensing & Analysis in Universities of Shandong, School of Chemistry and Chemical Engineering, University of Jinan, Jinan 250022, China

[‡]National Engineering Technology Research Center for Colloidal Materials, Shandong University, Jinan 250100, China

[§]Institute of Physical Chemistry, Polish Academy of Sciences, Kasprzaka 44/52, 01-224 Warsaw, Poland

ABSTRACT: A novel electrochemiluminescent (ECL) aptasensor was proposed for the determination of thrombin (TB) using exonuclease-catalyzed target recycling and hybridization chain reaction (HCR) to amplify the signal. The capture probe was immobilized on an Au-GS-modified electrode through a Au−S bond. Subsequently, the hybrid between the capture probe and the complementary thrombin binding aptamer (TBA) was aimed at obtaining double-stranded DNA (dsDNA). The interaction between TB and its aptamer led to the dissociation of dsDNA because TB has a higher affinity to TBA than the complementary strands. In the presence of exonuclease, aptamer was selectively digested and TB could be released for target recycling. Extended dsDNA was formed through HCR of the capture probe and two hairpin DNA strands (NH_2-DNA1 and NH_2-DNA1). Then, numerous europium multiwalled carbon nanotubes (Eu-MWCNTs) could be introduced through amidation reaction between NH_2-terminated DNA strands and carboxyl groups on the Eu-MWCNTs, resulting in an increased ECL signal. The multiple amplification strategies, including the amplification of analyte recycling and HCR, and high ECL efficiency of Eu-MWCNTs lead to a wide linear range (1.0×10^{-12}−5.0×10^{-9} mol/L) and a low detection limit (0.23 pmol/L). The method was applied to serum sample analysis with satisfactory results.

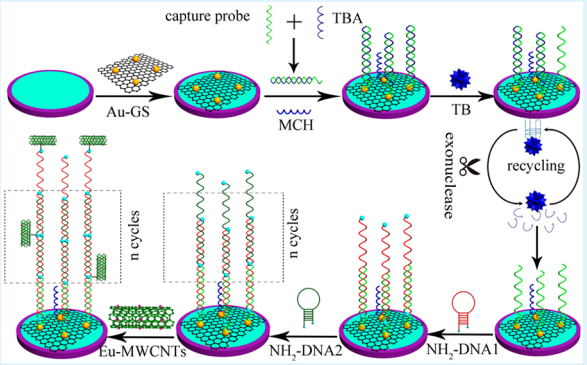

KEYWORDS: *aptasensor, Eu-MWCNTs, electrochemiluminescence, target recycling, thrombin*

INTRODUCTION

Aptamers are single-stranded DNA or RNA selectively attached to different target molecules with high affinity, including small molecules, drugs, and proteins. In comparison with the traditional molecular recognition system, aptamers are regarded as more competitive because of the simplicity of synthesis, ease of labeling, excellent stability, wide applicability, and high sensitivity. Various aptasensors based on electrochemistry,[1−3] fluorescence,[4−6] electrochemiluminescence (ECL)[7,8] and other assays[9] have been widely used in the determination of various biomolecules. Among them, as a kind of chemiluminescence (CL) produced by the electrochemical reaction, ECL has been proven to be a detection method with high sensitivity and selectivity in place of the traditional electrochemical and CL techniques.[10,11] Therefore, ECL-based aptasensors have attracted a great deal of attention recently because of the integrated advantages of ECL and aptamer with high specificity and affinity. At present, in order to further improve the sensitivity of sensors, various strategies have been developed including enzyme-free and -dependent amplification techniques.[12−14] For example, hybridization chain reaction (HCR) is an enzyme-free amplification technique by which the initiator can trigger hybridization and results in the polymerization of oligonucleotides into long nicked dsDNA polymers at mild conditions, which avoids the need of strict conditions to keep the activity of protein−enzyme. Therefore, HCR shows great potential in signal amplification.[15] Target recycling performed by enzymes such as DNAzymes, nicking enzymes, and exonucleases has also been proven as effective signal amplification.[16−19] With use of the catalytic nuclease in the sensor, further recycling and reuse of the target will be achieved that amplifies the detection signal. As mentioned above, two favorable methods, including exonuclease-catalyzed target recycling and HCR, were applied for signal amplification to fabricate an ECL-based aptasensor in this paper.

Multiwalled carbon nanotubes (MWCNTs), having a hollow structure, have received great attention for biological applications in drug delivery, biosensors, and so on.[20−22]

Received: December 29, 2014
Accepted: May 25, 2015
Published: May 25, 2015

DOI: 10.1021/acsami.5b03381
ACS Appl. Mater. Interfaces 2015, 7, 12663−12670

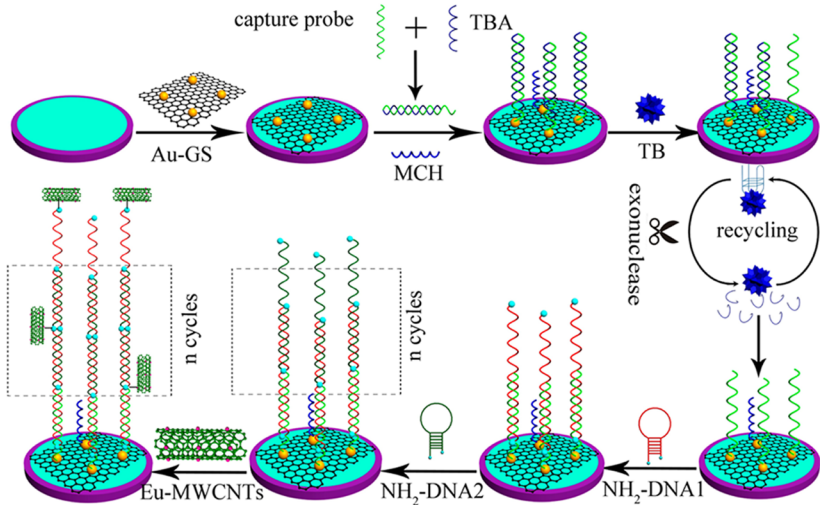

Figure 1. Schematic diagram of the proposed ECL-based aptasensor for TB detection.

However, carbon nanotubes (CNTs) are observed to exhibit weak IR emissions. As a result, luminescent CNTs functionalized with fluorescent materials must be synthesized in order to track and diagnose the effectiveness of the treatment. Compared with semiconductor quantum dots and organic fluorophores, the lanthanide-based luminescent probes are paid more and more attention because these kinds of probes have several merits. For example, lanthanide-doped nanocrystals show high quantum yields, superior photostability, and low toxicity, with their inherently long luminescence lifetimes preventing interference from any spontaneous background emission sources.[23,24] In our previous work, we successfully synthesized europium(III)-functionalized MWCNTs (denoted as Eu-MWCNTs), which showed both strong luminescent and anchoring properties. Europium(III) tris(2-theonyl)-trifluoroacetonate was coupled to MWCNTs through complex formation between europium(III) and bipyridine ligands.[25]

Usually, $Ru(bpy)_3^{2+}$[26,27] and luminol and its derivatives,[28,29] quantum dots[30−33] as ECL reagents, have been used to construct ECL sensors. Herein, using thrombin (TB) as a model analyte, we developed a highly sensitive aptasensor based on luminescent CNTs (Eu-MWCNTs) as a novel ECL reagent for determination of the protein. TB, a kind of serine protease, is composed of two polypeptide strands through cross-linking by disulfide bonds. It plays an essential role in several physiological and pathological processes, such as coagulation cascade, thrombosis, and hemostasis.[34] Generally, the normal concentration of TB ranges from nanomoles per liter to several micromoles per liter in blood during the coagulation process. So, the specific recognition and quantitative detection of TB is extremely important in both clinical practice and diagnostic application.

A schematic representation of the aptasensor with fabrication steps is shown in Figure 1. The aptamer was dissociated from the double-stranded DNA (dsDNA) with the presence of TB and selectively digested by exonuclease, which led to the release of TB for recycling of the analyte as well. Then, the extended dsDNA would be formed by the capture probe and two hairpin helpers through HCR on the electrode surface. Numerous ECL indicators, Eu-MWCNTs, thus can be efficiently introduced through an amidation reaction. On the basis of multiple signal amplification strategies, the proposed strategy exhibited a low detection limit of 0.23 pmol/L and a wide linear range from 1.0×10^{-12} to 5×10^{-9} mol/L for TB detection.

EXPERIMENTAL SECTION

Reagents. $RecJ_f$ (30 U/μL), purchased from New England Biolabs (Beijing) Ltd., is a single-stranded DNA specific exonuclease that catalyzes the removal of deoxynucleotide monophosphates from the 5′ terminus to the 3′ terminus of DNA. (3-Mercaptopropyl)-triethoxysilane (MPTES) was purchased from Aladdin Chemical Shanghai Co., Ltd. 1-Ethyl-3-[3-(dimethylamino)propyl]carbodiimide (EDC), $K_2S_2O_8$, 6-mercapto-1-hexanol (MCH), and *N*-hydroxysuccinimide (NHS) were obtained from Sinopharm Chemical Reagent Co., Ltd. (China). Hemoglobin (Hb), Immunoglobulin G (IgG), bovine serum albumin (BSA; 96−99%), and thrombin (TB) were purchased from Sigma (USA). All oligonucleotides were synthesized by Shanghai Sangon Biotech. Co., Ltd. (China), as shown in Table 1. Aptamer stock solutions were obtained by dissolving oligonucleotides in 20 mM Tris−HCl buffer (pH 7.4) containing 140 mM NaCl, 5.0 mM KCl, and 1.0 mM $MgCl_2$. Phosphate-buffered saline (PBS; 0.1 mol/L containing 0.1 mol/L NaCl, pH 7.4) was used as an electrolyte for all electrochemical measurements. Ultrapure water (18.25 MΩ cm, 24 °C) was used for all of the experiments.

Table 1. Sequence of Synthesized Oligonucleotides Used in This Work

name	oligonucleotide sequence
thrombin binding aptamer	5′-AAA **AGT CCG TGG TAG GGC AGG TTG GGG TGA CT**-$(CH_2)_6$-3′
capture probe	5′-SH-$(CH_2)_6$-AAT TGG **AGT CAC CCC AAC CTG CCC TAC CAC GGA CT**-3′
NH_2-DNA1	5′-NH_2-$(CH_2)_6$-**AGT CAC CCC AAC CTG CCC TAC CAC GGA CTT GAA ACA GTC CGT GGT AGG GCA GGT TGG GGT GAC TCC AAT T**-$(CH_2)_6$-NH_2-3′
NH_2-DNA2	5′-NH_2-$(CH_2)_6$-**GTT TCA AGT CCG TGG TAG GGC AGG TTG GGG TGA CTA ATT GGA GTC ACC CCA ACC TGC CCT ACC ACG GAC T**-$(CH_2)_6$-NH_2-3′

Apparatus. By employment of a MPI-F flow-injection CL detector, ECL measurements were operated (Xi'an Remax Electronic Science Technology Co. Ltd., China). With use of the three-electrode system composed of a platinum wire as the auxiliary electrode, an Ag/AgCl electrode as the reference electrode, and a glassy carbon electrode (GCE; 4 mm in diameter) as the working electrode, electrochemical measurements were performed on a CHI760D electrochemical workstation (Chenhua Instrument Shanghai Co. Ltd., China). The ECL spectrum of Eu-MWCNTs was measured

DOI: 10.1021/acsami.5b03381
ACS Appl. Mater. Interfaces 2015, 7, 12663−12670

using a BPCL-GPZ-TIC ultraweak luminscence analyzer (Institute of Biophysics, Chinese Academy of Sciences) in conjunction with a CHI760D electrochemical workstation. Electrochemical impedance spectroscopy (EIS) was acquired by the measurement unit of the impedance (IM6e, ZAHNER elektrik, Germany). Transmission electron microscopy (TEM) images were obtained by a Hitachi H-800 microscope (Japan). High-resolution TEM observations were performed on a JEOL-2100 microscope with an accelerating voltage of 200 kV. Confocal fluorescence microscopy observations were carried out using a Nikon D-Eclipse C1 controller combined with *EC-C1* software.

Preparation of Au-GS. Gold nanoparticles (Au NPs) were prepared by the reduction of $AuCl_4^-$ ions using sodium citrate according to the reported method.[35] In brief, a solution of $HAuCl_4$ (0.01 wt %, 100 mL) was heated to boiling, to which a solution of sodium citrate (1 wt %, 2.5 mL) was added. The boiling solution turned brilliant ruby red in ~15 min, indicating the formation of monodisperse spherical particles. The solution was then cooled to room temperature for further use.

Graphene oxide (GO) was synthesized by a modified Hummers method.[36] The typical procedure is as follows: GO dispersed in ethanol (1 wt %, 10 mL) was mixed with 0.2 mL of MPTES and heated to 70 °C under stirring for 1.5 h, and then 0.1 mL of 80% hydrazine hydrate was added under 95 °C for another 1.5 h. After drying in a vacuum, SH-GS was obtained.

A total of 10 mg of SH-GS was added to 10 mL of the prepared Au NP solution and further stirred for 12 h. Finally, the resulting Au-GS was isolated by centrifugation and dried in a vacuum.

Preparation of Eu-MWCNTs. As the starting materials, carboxylic-group-appended MWCNTs were first switched to acyl chloride-appended MWCNTs where amino-group-functionalized bipyridine was adhered by means of amide bond formation. In the end, with complex formation between europium(III) and bipyridine ligands, europium(III) tris(2-theonyl)trifluoroacetonate was coupled to MWCNTs. The detailed process was described in our previous work.[25]

Fabrication of the ECL Aptasensor. With the sequential use of 1.0, 0.3, and 0.05 μm alumina powder, a GCE was polished until a mirrorlike surface appeared and cleaned thoroughly before use. First of all, 6.0 μL of Au-GS solution (1.0 mg/mL) that was dispersed in chitosan (0.5 wt %) was add onto the electrode and dried. Then, 10 μL of a 2 μmol/L capture probe/aptamer mixture was attached to the electrode surface for 12 h at room temperature. After that, 5 μL of 2 mmol/L MCH was dripped onto the surface of the electrode for 1 h to eliminate the nonspecific binding effect and block the active groups that are left. Subsequently, 10 μL of TB with varying concentrations containing 0.15 U/μL of $RecJ_f$ exonuclease was added to the electrode surface and incubated for 40 min at 37 °C. After that, the electrode was incubated for 1 h with 10 μL of a mixture of hairpin probe NH2-DNA1 and NH2-DNA2 (1 μmol/L). Finally, the electrode was incubated for another 2 h in a Eu-MWCNT solution (1.5 mg/mL) containing EDC (50 mmol/L) and NHS (50 mmol/L). EDC and NHS were used to conjugate Eu-MWCNTs with NH_2-DNA1 and NH_2-DNA2 by the formation of an amide link between the amino of NH_2-DNA1 and NH_2-DNA2 and the carboxyl of Eu-MWCNTs. After washing, the electrode was ready for measurement.

ECL Detection of TB. The ECL behavior was monitored over a scanning range of −2.0 to 0 V in 10 mL of PBS containing 100 mmol/L $K_2S_2O_8$ at a photomultiplier tube voltage of 800 V and a scanning rate of 100 mV/s.

RESULTS AND DISCUSSION

Characterization of Au-GS and Eu-MWCNTs. Figure 2A shows a typical TEM image of the prepared Au-GS. It can be observed that a large number of Au NPs were successfully attached onto the surface of SH-GS with a wrinkled paperlike structure by interaction between Au NPs and −SH.

In this study, Eu-MWCNTs were used as ECL reagents. Because Eu^{3+} ions can serve as an indicative agent under fluorescence microscopy, the incorporation of Eu^{3+} ions can impart self-indicative advantages to CNTs. It can be seen from a typical fluorescence micrograph that Eu-MWCNTs show a bright red emission (the characteristic emission color of Eu^{3+} ions) by utilizing a filtered 365 nm UV laser, indicating that CNTs have been successfully modified with fluorescent Eu^{3+} functional groups.

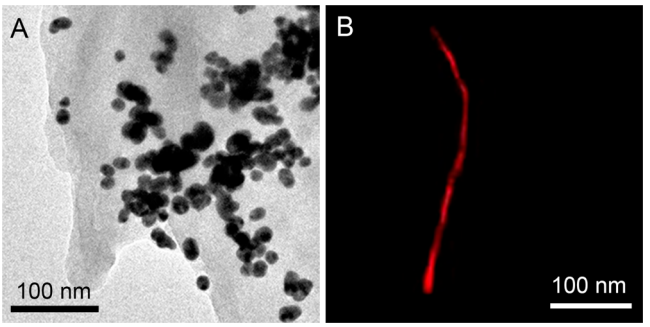

Figure 2. TEM image of Au-GS (A) and fluorescence microscopic image of Eu-MWCNTs with 365 nm UV-light excitation (B).

The ECL spectrum of Eu-MWCNTs was measured by inserting filters at wavelengths of 440, 460, 475, 490, 505, 520, 535, 555, 575, 590, 605, and 620 nm under cyclic volatammetry conditions. It can be seen from Figure 3 that three peaks were found in the region between 500 and 650 nm and commonly associated with $^5D_0 \rightarrow {}^7F_J$ transitions of Eu^{3+}.[37−39]

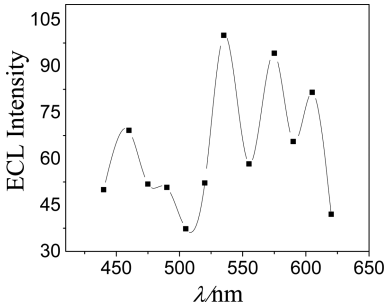

Figure 3. ECL spectrum of Eu-MWCNTs.

Amplification Performance of the Proposed Aptasensor. As shown in Figure 4, in order to assess whether the signal response would be efficiently amplified by the $RecJ_f$ exonuclease, ECL responses with and without exonuclease were both studied. Curve a shows that the ECL intensity is low without the target TB. As expected, curve c exhibits a

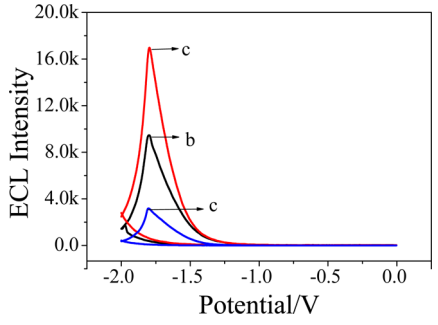

Figure 4. ECL intensity−potential curves without TB and exonuclease (a) in the absence (b) and presence (c) of exonuclease for TB (5.0×10^{-9} mol/L) detection.

DOI: 10.1021/acsami.5b03381
ACS Appl. Mater. Interfaces 2015, 7, 12663−12670

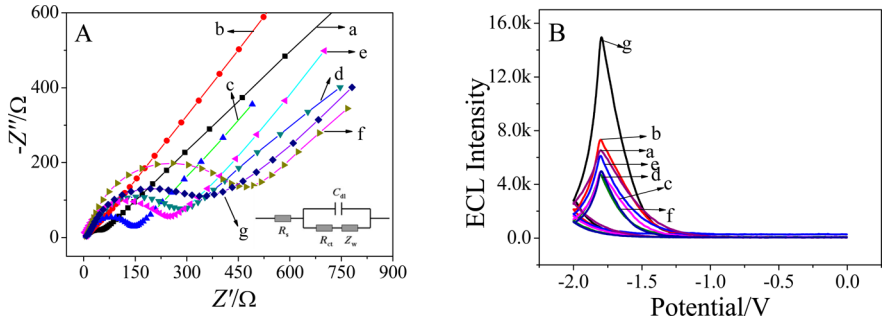

Figure 5. EIS in the presence of a 5.0 mmol/L $[Fe(CN)_6]^{3-/4-}$ solution containing 0.1 mol/L KCl (A) and ECL intensity−potential curves in PBS containing 100 mmol/L $K_2S_2O_8$ with a potential range of −2.0 to 0 V (B): (a) bare GCE; (b) Au-GS/GCE; (c) dsDNA of the capture probe and aptamer/Au-GS/GCE; (d) MCH/dsDNA of the capture probe and aptamer/Au-GS/GCE; (e) a mixture of TB and exonuclease/MCH/dsDNA of the capture probe and aptamer/Au-GS/GCE; (f) NH_2-DNA1 and NH_2-DNA2/mixture of TB and exonuclease/MCH/dsDNA of the capture probe and aptamer/Au-GS/GCE; (g) Eu-MWCNTs/NH_2-DNA1 and NH_2-DNA2/mixture of TB and exonuclease/MCH/dsDNA of the capture probe and aptamer/Au-GS/GCE.

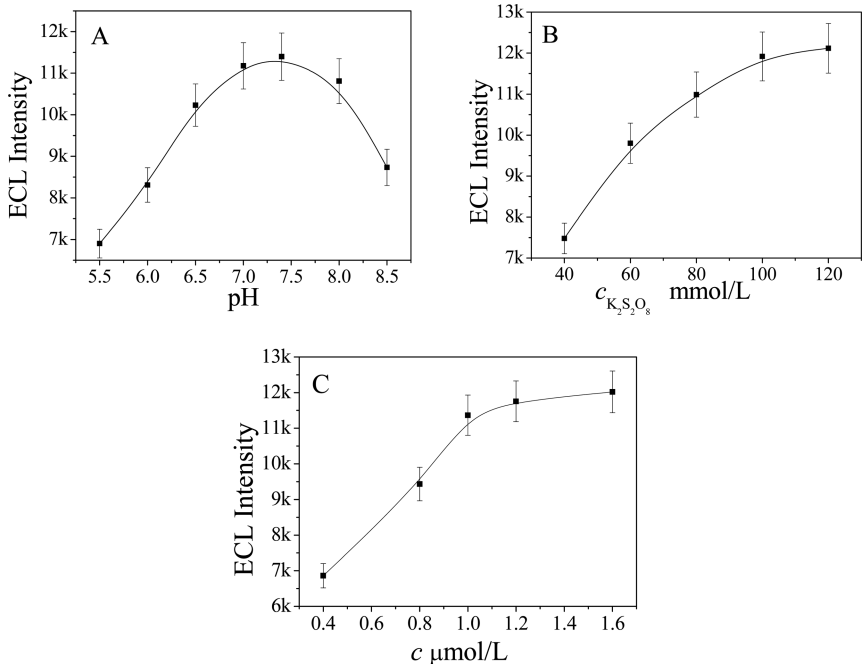

Figure 6. Effect of the pH (A), the concentration of $K_2S_2O_8$ (B), and the concentrations of NH_2-DNA1 and NH_2-DNA2 (C) on the response of the aptasensor for detection of 1.0×10^{-10} mol/L TB. Error bars represent standard deviations of five parallel experiments.

considerable increase in the ECL response compared with curve b. This means that with the appearance of exonuclease an apparent increase of the signal is observed, demonstrating the excellent amplification performance of $RecJ_f$ exonuclease.

Characterization of the Modified Electrode. EIS is effectively used to probe the features of the modified electrode surface. There is a semicircle and a linear portion in the impedance spectra. The semicircle diameter at higher frequencies agrees with the resistance to electron transfer, and the linear part at lower frequencies remains with the diffusion process. The semicircle diameter equals the charge-transfer resistance (R_{ct}). EIS was measured in the frequency range of 0.1−10^5 Hz. Figure 5A illustrates the EIS of different electrodes in the presence of a 5.0 mmol/L $[Fe(CN)_6]^{3-/4-}$ solution containing 0.1 mol/L KCl. When Au-GS was modified on the electrode, the resistance obviously decreased (curve b) compared with that of the bare GCE (curve a). The reason was that Au-GS as an excellent conducting material could facilitate electron transfer. After incubation with dsDNA of capture probe and aptamer, the semicircle increased remarkably (curve c) because dsDNA was successfully fixed on the electrode and hindered electron transfer. After that, a larger semicircle diameter in curve d was observed, indicating that the nonconductive MCH blocked the high resistance of the electrode interface to the prepared aptasensors. Subsequently, R_{ct} decreased again (curve e) after incubation with a mixture of TB and exonuclease. The reason was that the constitution of aptamer TB would not only dissociate the aptamer from the dsDNA but also liberate TB for recycling by $RecJ_f$ exonuclease and thus dissociate more nonelectroactive aptamers. A large semicircle domain is observed when the electrode was incubated with NH_2-DNA1 and NH_2-DNA2 (curve f), which indicates the successful capture of NH_2-DNA1 and NH_2-DNA2, blocking electron transfer. When Eu-MWCNTs were immobilized, R_{ct} decreased greatly (curve g) because of its excellent conducting property, which made electron-transfer easier. The equivalent circuit, containing the resistance of the solution (R_s), R_{ct}, the Warburg impedance (Z_W), and the

DOI: 10.1021/acsami.5b03381
ACS Appl. Mater. Interfaces 2015, 7, 12663−12670

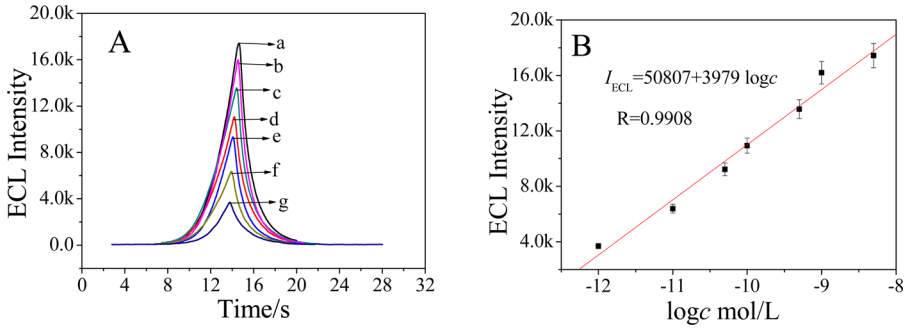

Figure 7. ECL response of the aptasensor to different concentrations of TB (A), from a to g: 5×10^{-9}, 1.0×10^{-9}, 5×10^{-10}, 1.0×10^{-10}, 5×10^{-11}, 1.0×10^{-11}, and 1.0×10^{-12} mol/L. Calibration curve of the aptasensor for different concentrations of TB (B).

double-layer capacitance (C_{dl}), is shown in the inset of Figure 5A.

The stepwise construction process of the aptasensor was also characterized by ECL. The ECL intensity−potential curves were obtained by different modified electrodes in PBS containing 100 mmol/L $K_2S_2O_8$, as shown in Figure 5B. Compared with the bare electrode (curve a), the ECL response was enhanced after Au-GS was immobilized on it (curve b). Subsequently, an obvious decrease in the ECL signal was obtained (curve c) when dsDNA of the capture probe and aptamer was conjugated to the electrode surface. The reason was that dsDNA obstructed electron transport. Followed by the employment of MCH to block nonspecific binding sites, a small decrease of the ECL signal was detected (curve d) because MCH is a nonconductive small molecule. After incubation with a mixture of TB and exonuclease, the ECL signal increased again (curve e). The reason was that more nonelectroactive aptamers left the electrode surface. The ECL signal (curve f) decreased after NH_2-DNA1 and NH_2-DNA2 were successfully immobilized, which could be attributed to the hindrance of two hairpin DNA strands. A quite high ECL signal (curve g) was observed after Eu-MWCNTs were coated on the modified electrode, indicating that they were good ECL luminophores.

On the basis of the above results, we can confirm that the electrode was well-modified.

Optimization of the Experimental Conditions. To achieve an optimal ECL signal, the pH value of the substrate solution was investigated. The effect of the pH on the ECL intensity was tested over a pH range from 5.5 to 8.5 at constant concentrations of TB. As shown in Figure 6A, the ECL intensity increased with an increase of the pH from 5.5 to 7.4 and reached a maximum. After that, when the pH varied from 7.4 to 8.5, the ECL intensity decreased accordingly. Therefore, pH 7.4 was regarded as the optimal value for ECL response. In an acidic solution, the reduction of proton to hydrogen would take place at an applied negative potential, which might inhibit the reduction of $S_2O_8^{2-}$. However, the intermediate $SO_4^{\bullet-}$ from $S_2O_8^{2-}$ reduction would be scavenged by $OH^{\bullet-}$, leading to a decrease in the ECL intensity in a basic solution.[40] Figure 6B shows the effect of the coreactant $K_2S_2O_8$ concentration in the substrate solution on the ECL intensity. The ECL intensity increased with increasing $K_2S_2O_8$ concentration from 40 to 100 mmol/L because more $(Eu^{3+})^*$ was produced from oxidation of Eu^{2+} by the electrogenerated $SO_4^{\bullet-}$ and remained constant in the range 100−120 mmol/L. Therefore, 100 mmol/L $K_2S_2O_8$ was chosen to ensure adequate sensitivity and to save the dosage.

To verify the signal amplification effect of HCR, the effect of the NH_2-DNA1 and NH_2-DNA2 concentrations on the ECL intensity was also tested at constant concentrations of TB. As shown in Figure 6C, it can be seen that ECL responses increase dramatically at a concentration of less than 1 μmol/L and remain nearly stable after that. Thus, the concentrations of NH_2-DNA1 and NH_2-DNA2 are selected as 1 μmol/L, and after that, the hybridization of NH_2-DNA1 with NH_2-DNA2 was exhausted. The above analysis confirmed that HCR indeed played an important role in the improvement of the response signal intensity.

To obtain steady ECL signals, the aptasensor needed to be incubated with TB of different concentrations, and the ECL responses were recorded by scanning continuously. The ECL response increased with an increase of the TB concentration from 1.0×10^{-12} to 5.0×10^{-9} mol/L (as shown in Figure 7A), with a detection limit of 0.23 pmol/L based on S/N = 3. The regression equation was I_{ECL} = 50807 + 3979 log c with a correlation coefficient of 0.9908 (as shown in Figure 7B).

From Table 2, it can be seen that the detection limit and linear range using Eu-MWCNTs are better or comparable to the results reported for the determination of TB.

Table 2. Comparison of the Proposed Aptasensor with Other Reported Aptasensors for TB

analytical method	linear range (nmol/L)	detection limit (pmol/L)	reference
ECL	0.001−1	0.38	41
EIS[a]	0.0047−0.5	4.4	42
PCL[b]	0.25−5	80	43
ECL	0.2−200	60	44
DPV[c]	0.001−0.5	0.5	45
ECL	0.001−5	0.23	this work

[a]Electrochemical impedance spectroscopy. [b]Photoinduced chemiluminescence. [c]Differential pulse voltammetry.

Possible Mechanism of ECL Aptasensors. According to the experimental results, the possible mechanism of the present ECL system was described as follows:[39,46,47] as the electrode was scanned from −2.0 to 0 V, it was easy to reduce Eu^{3+} ions to Eu^{2+} (eq 1). Meanwhile, with enough negative potential, $S_2O_8^{2-}$ was reduced to $SO_4^{\bullet-}$ and SO_4^{2-} (eq 2). Under further reaction of the strong oxidant $SO_4^{\bullet-}$ with Eu^{2+}, the excited state $(Eu^{3+})^*$ (eq 3) was generated by electron transfer in the aqueous solution. As $(Eu^{3+})^*$ turned from the excited state to the ground state (eq 4), light was emitted and detected.

$$Eu^{3+} + e^- \rightarrow Eu^{2+} \quad (1)$$

DOI: 10.1021/acsami.5b03381
ACS Appl. Mater. Interfaces 2015, 7, 12663−12670

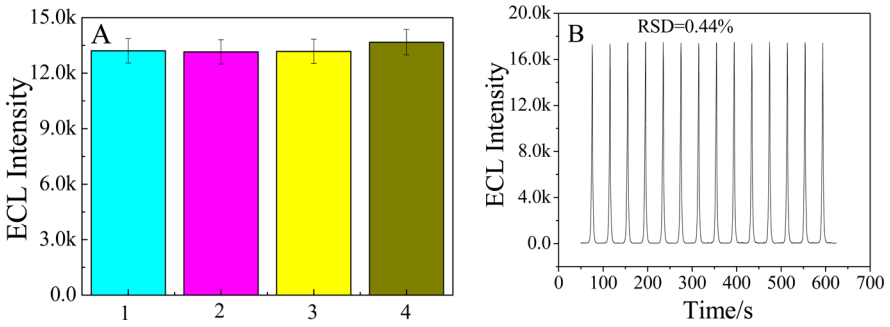

Figure 8. Selectivity of the aptasensor (A): 50 mmol/L BSA + 0.5 nmol/L TB (1); 50 mmol/L Hb + 0.5 nmol/L TB (2); 50 mmol/L IgG + 0.5 nmol/L TB (3); 0.5 nmol/L TB (4). Error bar = RSD (n = 5). The stability of the aptasensor incubated with 5 nmol/L TB under continuous potential scanning for 14 cycles (B).

$$S_2O_8^{2-} + e^- \rightarrow SO_4^{\bullet -} + SO_4^{2-} \quad (2)$$

$$SO_4^{\bullet -} + Eu^{2+} \rightarrow SO_4^{2-} + (Eu^{3+})^* \quad (3)$$

$$(Eu^{3+})^* \rightarrow Eu^{3+} + h\nu \quad (4)$$

Reproducibility, Selectivity, and Stability. To assess the reproducibility of the aptasensor, a series of five electrodes were prepared for the determination of 5×10^{-9} mol/L TB. With 1.6% as the relative standard deviation (RSD) of the measurements for the five electrodes, the reproducibility of the proposed aptasensor was proven to be excellent.

The selectivity of the aptasensor was studied as well. A 0.5 nmol/L TB solution containing 50 nmol/L interfering substances (BSA, Hb, and IgG) was measured by the aptasensor, and the results are shown in Figure 8A. The ECL intensity exhibited no remarkable change. The current variation due to the interfering substances was less than 1.9% of that without interferences, indicating that the interferences of the relatively high concentrations had negligible effects on TB detection, and the selectivity of the proposed aptasensor was acceptable.

The stability of the ECL responses of the aptasensor was evaluated under continuous potential scanning for 14 cycles. As can be seen in Figure 8B, stable and high signals were observed, demonstrating that the constructed sensor possessed good stability and was suitable for ECL detection. The storage stability of the aptasensor was also examined by storing it in PBS at 4 °C when not in use, and at different storage periods, the aptasensor was used to detect the same concentration of TB. The results indicate that the aptasensor retained 97.7% of its initial response after 5 days of storage and its response decreased to 92.6% after 10 days.

Real Sample Analysis. The amount of TB in the human serum sample was measured three times, and the RSD was calculated to obtain the precision. The accuracy was also studied through a recovery experiment using the standard addition method. An appropriate amount of the TB standard solution was added to the corresponding samples. With the same experiments conducted three times, the average recovery was calculated. As is shown Table 3, the RSD is 2.4% and the recovery is 96.8%. Thus, the proposed aptasensor could be satisfactorily applied to the determination of TB in real biological samples.

Table 3. Results for the Determination of TB in the Human Serum Sample

sample	content of TB (nmol/L)	average (n = 3, nmol/L)	added (nmol/L)	recovery value (nmol/L)	RSD (%)	recovery (n = 3, %)
human serum	0.589		0.500	0.480		
	0.618	0.603	0.500	0.534	2.4	96.8
	0.603		0.500	0.442		

CONCLUSIONS

An ultrasensitive ECL aptasensor with Eu-MWCNTs as luminophores to detect TB was developed. With the use of exonuclease-catalyzed target recycling and HCR for signal amplification, the sensitivity of the proposed aptasensor could be further improved. First, by means of exonuclease-catalyzed target recycling, a great deal of single-stranded capture probes could be obtained. Second, through HCR, a mass of NH_2-DNA1 and NH_2-DNA2 would be fixed on the electrode surface. As a result, plenty of Eu-MWCNTs could be attached to these dsDNAs by amidation reaction, producing an amplified ECL signal. Thus, this developed aptasensor showed high sensitivity, good selectivity and reproducibility, and acceptable stability. Moreover, there would be a promising future for the proposed platform in clinical applications to detect TB, and a series of ECL aptasensors for other targets could be similarly developed based on the principle of signal amplification and aptasensor.

AUTHOR INFORMATION

Corresponding Author

*Tel.: +86 531 82765730. Fax: +86 531 82765969. E-mail: sdjndxwq@163.com.

Notes

The authors declare no competing financial interest.

ACKNOWLEDGMENTS

This study was supported by the Natural Science Foundation of China (Grants 21405059 and 21203109), Shandong Province (Grant ZR2014BL024), and University of Jinan (Grant XKY1405). R.H. acknowledges support through National Science Center Grant Opus 4UMO-2012/07/B/ST4/01400. Q.W. thanks the Special Foundation for Taishan Scholar Professorship of Shandong Province and University of Jinan.

REFERENCES

(1) Zhao, J.; He, X.; Bo, B.; Liu, X.; Yin, Y.; Li, G. A "Signal-on" Electrochemical Aptasensor for Simultaneous Detection of Two Tumor Markers. *Biosens. Bioelectron.* **2012**, *34*, 249−252.

DOI: 10.1021/acsami.5b03381
ACS Appl. Mater. Interfaces 2015, 7, 12663−12670

(2) Kashefi-Kheyrabadi, L.; Mehrgardi, M. A. Aptamer-based Electrochemical Biosensor for Detection of Adenosine Triphosphate Using a Nanoporous Gold Platform. *Bioelectrochemistry* **2013**, *94*, 47−52.
(3) Li, L. D.; Mu, X. J.; Peng, Y.; Chen, Z. B.; Guo, L.; Jiang, L. Signal-on Architecture for Electrochemical Aptasensors Based on Multiple Ion Channels. *Anal. Chem.* **2012**, *84*, 10554−10559.
(4) Xu, Z.; Sato, Y.; Nishizawa, S.; Teramae, N. Fluorescent Aptasensors Based on Conformational Adaptability of Abasic Site-containing Aptamers in Combination with Abasic Site-binding Ligands. *Biosens. Bioelectron.* **2011**, *26*, 4733−4738.
(5) Zheng, A. X.; Wang, J. R.; Li, J.; Song, X. R.; Chen, G. N.; Yang, H. H. Enzyme-free Fluorescence Aptasensor for Amplification Detection of Human Thrombin via Target-catalyzed Hairpin Assembly. *Biosens. Bioelectron.* **2012**, *36*, 217−221.
(6) Wu, S.; Duan, N.; Ma, X.; Xia, Y.; Wang, H.; Wang, Z.; Zhang, Q. Multiplexed Fluorescence Resonance Energy Transfer Aptasensor between Upconversion Nanoparticles and Graphene Oxide for the Simultaneous Determination of Mycotoxins. *Anal. Chem.* **2012**, *84*, 6263−6270.
(7) Chai, Y.; Tian, D.; Cui, H. Electrochemiluminescence Biosensor for the Assay of Small Molecule and Protein based on Bifunctional Aptamer and Chemiluminescent Functionalized Gold Nanoparticles. *Anal. Chim. Acta* **2012**, *715*, 86−92.
(8) Hu, L.; Bian, Z.; Li, H.; Han, S.; Yuan, Y.; Gao, L.; Xu, G. $[Ru(bpy)_2dppz]^{2+}$ Electrochemiluminescence Switch and its Applications for DNA Interaction Study and Label-free ATP Aptasensor. *Anal. Chem.* **2009**, *81*, 9807−9811.
(9) Du, F.; Alam, M. N.; Pawliszyn, J. Aptamer-functionalized Solid Phase Microextraction−Liquid Chromatography/Tandem Mass Spectrometry for Selective Enrichment and Determination of Thrombin. *Anal. Chim. Acta* **2014**, *845*, 45−52.
(10) Xu, S.; Liu, Y.; Wang, T.; Li, J. Highly Sensitive Electrogenerated Chemiluminescence Biosensor in Profiling Protein Kinase Activity and Inhibition Using Gold Nanoparticle as Signal Transduction Probes. *Anal. Chem.* **2010**, *82*, 9566−9572.
(11) Deng, S.; Hou, Z.; Lei, J.; Lin, D.; Hu, Z.; Yan, F.; Ju, H. Signal Amplification by Adsorption-induced Catalytic Reduction of Dissolved Oxygen on Nitrogen-doped Carbon Nanotubes for Electrochemiluminescent Immunoassay. *Chem. Commun.* **2011**, *47*, 12107−12109.
(12) Lei, J.; Ju, H. Signal Amplification Using Functional Nanomaterials for Biosensing. *Chem. Soc. Rev.* **2012**, *41*, 2122−2134.
(13) Bi, S.; Li, L.; Zhang, S. Triggered Polycatenated DNA Scaffolds for DNA Sensors and Aptasensors by a Combination of Rolling Circle Amplification and DNAzyme Amplification. *Anal. Chem.* **2010**, *82*, 9447−9454.
(14) Gao, F.; Lei, J.; Ju, H. Assistant DNA Recycling with Nicking Endonuclease and Molecular Beacon for Signal Amplification Using a Target-complementary Arched Structure. *Chem. Commun.* **2013**, *49*, 4006−4008.
(15) Hun, X.; Xu, Y.; Chen, C. DNA-based hybridization Chain Reaction for Signal Amplification and Ultrasensitive Chemiluminescence Detection of Gibberellic Acid. *Sens. Actuators B* **2014**, *202*, 594−599.
(16) Tong, P.; Zhang, L.; Xu, J. J.; Chen, H. Y. Simply Amplified Electrochemical Aptasensor of Ochratoxin A Based on Exonuclease-catalyzed Target Recycling. *Biosens. Bioelectron.* **2011**, *29*, 97−101.
(17) Chen, Y.; Jiang, B.; Xiang, Y.; Chai, Y.; Yuan, R. Target Recycling Amplification for Sensitive and Label-free Impedimetric Genosensing Based on Hairpin DNA and Graphene/Au Nanocomposites. *Chem. Commun.* **2011**, *47*, 2798−2800.
(18) Fan, Q.; Zhao, J.; Li, H.; Zhu, L.; Li, G. Exonuclease III-based and Gold Nanoparticle-assisted DNA Detection with Dual Signal Amplification. *Biosens. Bioelectron.* **2012**, *33*, 211−215.
(19) Gao, F.; Lei, J.; Ju, H. Ultrasensitive Fluorescence Detection of Bleomycin Via Exonuclease III-aided DNA Recycling Amplification. *Chem. Commun.* **2013**, *49*, 7561−7563.
(20) Yang, S.; Yin, Y.; Li, G.; Yang, R.; Li, J.; Qu, L. Immobilization of Gold Nanoparticles on Multi-wall Carbon Nanotubes as an Enhanced Material for Selective Voltammetric Determination of Dopamine. *Sens. Actuators B* **2013**, *178*, 217−221.
(21) Boncel, S.; Zając, P.; Koziol, K. K. K. Liberation of Drugs from Multi-wall Carbon Nanotube Carriers. *J. Controlled Release* **2013**, *169*, 126−140.
(22) Esnaashari, F.; Moghadam, M.; Mirkhani, V.; Tangestaninejad, S.; Mohammadpoor-Baltork, I.; Khosoropour, A. R.; Zakeri, M.; Hushmandrad, S. $MoO_2(acac)_2$ Supported on Multi-wall Carbon Nanotubes: Highly Efficient and Reusable Catalysts for Alkene Epoxidation with *tert*-BuOOH. *Polyhedron* **2012**, *48*, 212−220.
(23) Chen, B.; Zhang, H.; Du, N.; Zhang, B.; Wu, Y.; Shi, D.; Yang, D. Magnetic−fluorescent Nanohybrids of Carbon Nanotubes Coated with Eu, Gd Co-doped LaF_3 as a Multimodal Imaging Probe. *J. Colloid Interface Sci.* **2012**, *367*, 61−66.
(24) Picot, A.; D'Aléo, A.; Baldeck, P. L.; Grichine, A.; Duperray, A.; Andraud, C.; Maury, O. Long-lived Two-photon Excited Luminescence of Water-soluble Europium Complex: Applications in Biological Imaging Using Two-photon Scanning Microscopy. *J. Am. Chem. Soc.* **2008**, *130*, 1532−1533.
(25) Xin, X.; Pietraszkiewicz, M.; Pietraszkiewicz, O.; Chernyayeva, O.; Kalwarczyk, T.; Gorecka, E.; Pociecha, D.; Li, H. Eu(III)-coupled Luminescent Multi-walled Carbon Nanotubes in Surfactant Solutions. *Carbon* **2012**, *50*, 436−443.
(26) Qi, W.; Liu, Z.; Lai, J.; Gao, W.; Liu, X.; Xu, M.; Xu, G. Detection of Ozone Based on its Striking Inhibition of Tris(1,10-phenanthroline)ruthenium(II)/Glyoxal Electrochemiluminescence. *Chem. Commun.* **2014**, *50*, 8164−8166.
(27) Ballesta-Claver, J.; Rodríguez-Gómez, R.; Capitán-Vallvey, L. F. Disposable Biosensor Based on Cathodic Electrochemiluminescence of Tris(2,2-bipyridine)ruthenium(II) for Uric Acid Determination. *Anal. Chim. Acta* **2013**, *770*, 153−160.
(28) Zhao, H. F.; Liang, R. P.; Wang, J. W.; Qiu, J. D. One-pot Synthesis of GO/AgNPs/Luminol Composites with Electrochemiluminescence Activity for Sensitive Detection of DNA Methyltransferase Activity. *Biosens. Bioelectron.* **2015**, *63*, 458−464.
(29) Haghighi, B.; Bozorgzadeh, S. Enhanced Electrochemiluminescence from Luminol at Multi-walled Carbon Nanotubes Decorated with Palladium Nanoparticles: A Novel Route for the Fabrication of an Oxygen Sensor and a Glucose Biosensor. *Anal. Chim. Acta* **2011**, *697*, 90−97.
(30) Hu, X.; Zhang, X.; Jin, W. Applications of Electrochemiluminescence Resonance Energy Transfer between CdSe/ZnS Quantum Dots and Cyanine Dye (Cy5) Molecules in Evaluating Interactions and Conformational Changes of DNA Molecules. *Electrochim. Acta* **2013**, *94*, 367−373.
(31) Jie, G.; Zhao, Y.; Niu, S. Amplified electrochemiluminescence detection of cancer cells using a New Bifunctional Quantum Dot as Signal Probe. *Biosens. Bioelectron.* **2013**, *50*, 368−372.
(32) Divsar, F.; Ju, H. Electrochemiluminescence Detection of Near Single DNA Molecules by using Quantum Dots−dendrimer Nanocomposites for Signal Amplification. *Chem. Commun.* **2011**, *47*, 9879−9881.
(33) Wang, J.; Zhao, W. W.; Li, X. R.; Xu, J. J.; Chen, H. Y. Potassium-doped Graphene Enhanced Electrochemiluminescence of SiO_2@CdS Nanocomposites for Sensitive Detection of TATA-binding Protein. *Chem. Commun.* **2012**, *48*, 6429−6431.
(34) Bock, L. C.; Griffin, L. C.; Latham, J. A.; Vermaas, E. H.; Toole, J. J. Selection of Single Stranded DNA Molecules that Bind and Inhibit Human Thrombin. *Nature* **1992**, *355*, 564.
(35) Frens, G. Controlled Nucleation for the Regulation of the Particle Size in Monodisperse Gold Suspensions. *Nat. Phys. Sci.* **1973**, *241*, 20−22.
(36) Marcano, D. C.; Kosynkin, D. V.; Berlin, J. M.; Sinitskii, A.; Sun, Z.; Slesarev, A.; Alemany, L. B.; Lu, W.; Tour, J. M. Improved Synthesis of Graphene Oxide. *ACS Nano* **2010**, *4*, 4806−4814.
(37) Staninski, K.; Kaczmarek, M.; Lis, S.; Komar, D.; Szyczewski, A. Spectral Analysis in Ultraweak Emissions of Chemi- and Electrochemiluminescence Systems. *J. Rare Earths* **2009**, *27*, 593−597.

DOI: 10.1021/acsami.5b03381
ACS Appl. Mater. Interfaces 2015, 7, 12663−12670

(38) Kim, W. J.; Gwag, J. S.; Kang, J. G.; Sohn, Y. Photoluminescence Imaging of Eu(III), Eu(III)/Ag, Eu(III)/Tb(III), and Eu(III)/Tb(III)/Ag-doped $Gd(OH)_3$ and Gd_2O_3 Nanorods. *Ceram. Int.* **2014**, *40*, 12035−12044.
(39) Bregolin, F. L.; Franzen, P.; Boudinov, H.; Sias, U. S.; Behar, M. Low Temperature and Decay Lifetime Photoluminescence of Eu and Tb Nanoparticles Embedded into SiO_2. *J. Lumin.* **2014**, *153*, 144−147.
(40) Yang, S.; Liang, J.; Luo, S.; Liu, C.; Tang, Y. Supersensitive Detection of Chlorinated Phenols by Multiple Amplification Electrochemiluminescence Sensing Based on Carbon Quantum Dots/Graphene. *Anal. Chem.* **2013**, *85*, 7720−7725.
(41) Yu, X.; Cui, H. Electrochemiluminescence Bioassay for Thrombin Based on Dynamic Assembly of Aptamer, Thrombin and *N*-(aminobutyl)-*N*-(ethylisoluminol) Functionalized Gold Nanoparticles. *Electrochim. Acta* **2014**, *125*, 156−162.
(42) Xu, H.; Gorgy, K.; Gondran, C.; Goff, A. L.; Spinelli, N.; Lopez, C.; Defrancq, E.; Cosnier, S. Label-free Impedimetric Thrombin Sensor Based on Poly(pyrrole-nitrilotriacetic acid)−aptamer Film. *Biosens. Bioelectron.* **2013**, *41*, 90−95.
(43) Jiang, Z.; Yang, T.; Liu, M.; Hu, Y.; Wang, J. An Aptamer-based Biosensor for Sensitive Thrombin Detection with Phthalocyanine@SiO_2 Mesoporous Nanoparticles. *Biosens. Bioelectron.* **2014**, *53*, 340−345.
(44) Li, Y.; Qi, H.; Peng, Y.; Gao, Q.; Zhang, C. Electrogenerated Chemiluminescence Aptamer-based Method for the Determination of Thrombin Incorporating Quenching of Tris(2,2′-bipyridine)ruthenium by Ferrocene. *Electrochem. Commun.* **2008**, *10*, 1322−1325.
(45) Liu, X.; Li, Y.; Zheng, J.; Zhang, J.; Sheng, Q. Carbon Nanotube-enhanced Electrochemical Aptasensor for the Detection of Thrombin. *Talanta* **2010**, *81*, 1619−1624.
(46) Staninski, K.; Lis, S. Ultraweak Emission of the Eu(III) Ions in Cathodic Generated Electrochemiluminescence. *Opt. Mater.* **2011**, *33*, 1540−1543.
(47) Deng, L.; Du, Y.; Xu, J.; Chen, H. An off−on−off Electrochemiluminescence Approach for Ultrasensitive Detection of Thrombin. *Biosens. Bioelectron.* **2014**, *59*, 58−63.

DOI: 10.1021/acsami.5b03381
ACS Appl. Mater. Interfaces 2015, 7, 12663−12670